The real-time performance of a two-dimensional ANC barrier using a DSP and common audio equipment

Christian Kleinhenrich, Tobias Weigler and Detlef Krahé
University of Wuppertal, Rainer-Gruenter-Str. 21, 42119 Wuppertal, Germany

Summary
The paper deals with a two-dimensional Active Noise Control (ANC) system in a linear setup to be used as an active sound barrier. Common audio equipment in combination with a Texas Instruments C6455 fixed point digital signal processor (DSP) was used to construct this multiple input multiple output (MIMO) system. Appropriate ANC algorithms can be achieved in different ways by using model based approaches or adaptive techniques. Also combinations are possible. Usually, pressure and velocity or pressure and pressure gradient microphones are combined as reference sensors in such a system. The paper presents the system setup and the underlying algorithms. It is demonstrated that the application of cardioid reference microphones is sufficient instead of using a combination of omnidirectional and bi-directional sensors. Additionally, measurement results are presented to evaluate the real-time performance of the system for band-pass filtered primary noise.

PACS no. 43.50.+y

1. System setup

The presented two-dimensional feedforward Active Noise Control (ANC) system uses reference sensors in a linear arrangement to measure a given sound field, the primary field. These sensors consist of six microphones with a cardioid characteristic. Six speakers form a line parallel to the line of the reference sensors to synthesize a secondary field, which is to damp the primary field. A third parallel line of six omnidirectional microphones can be used for error sensing. The line of reference and the line of error sensors are both 0,7 m away from the line of secondary sources. A drawing of the system arrangement in the semi-anechoic chamber of the University of Wuppertal is given in figure 1. It also shows the position of the primary source that produces the unwanted noise. Hence, the quiet zone shall be to the right of the secondary sources.

The digital signal processing of this multiple input multiple output (MIMO) system is accomplished by a Texas Instruments TMX320C6455+ DSP on a Spectrum Digital TMS320C6455 DSP Starter Kit (DSK6455) [1, 2]. The TMX320C6455+ is a beta version of the TMS320C6455+. Formerly, pairs of electret microphones were used as reference sensors in combination with in-house built microphone preamps. A DSK6455 daughter card with 24 analog input and 12 analog output channels was built for the conversation between analog and digital signals with a resolution of 16 bit and a sampling rate of 44 kHz. Additionally, cables with non-standard connectors were used within the system for signal transfers and the power supply of the microphone preamps. Gradually, these parts became more and more unreliable and repairs were costly and time-consuming. Therefore, a different approach was needed.

1.1. Revised setup

The aim was to rebuild the system by using as much commercially available audio equipment and standard cables as possible. First, the electret capsules were replaced by large-diaphragm condenser microphones of type AKG Perception 420. The Perception 420 can be used as omni-directional, figure-eight or cardioid receiver. One benefit is, that both capsules of the condenser microphone are calibrated by the producer, since the calibration of the electret microphone pairs within the system caused problems in the past.

Next, the in-house built preamps and converters were substituted by three Focusrite OctoPre MkII Dynamic. These devices offer 8 microphone preamps and A/D-convertes, 8 D/A-converters with line outputs and an ADAT interface. The OctoPre MkII Dynamic were chosen because of relatively low conversion la-

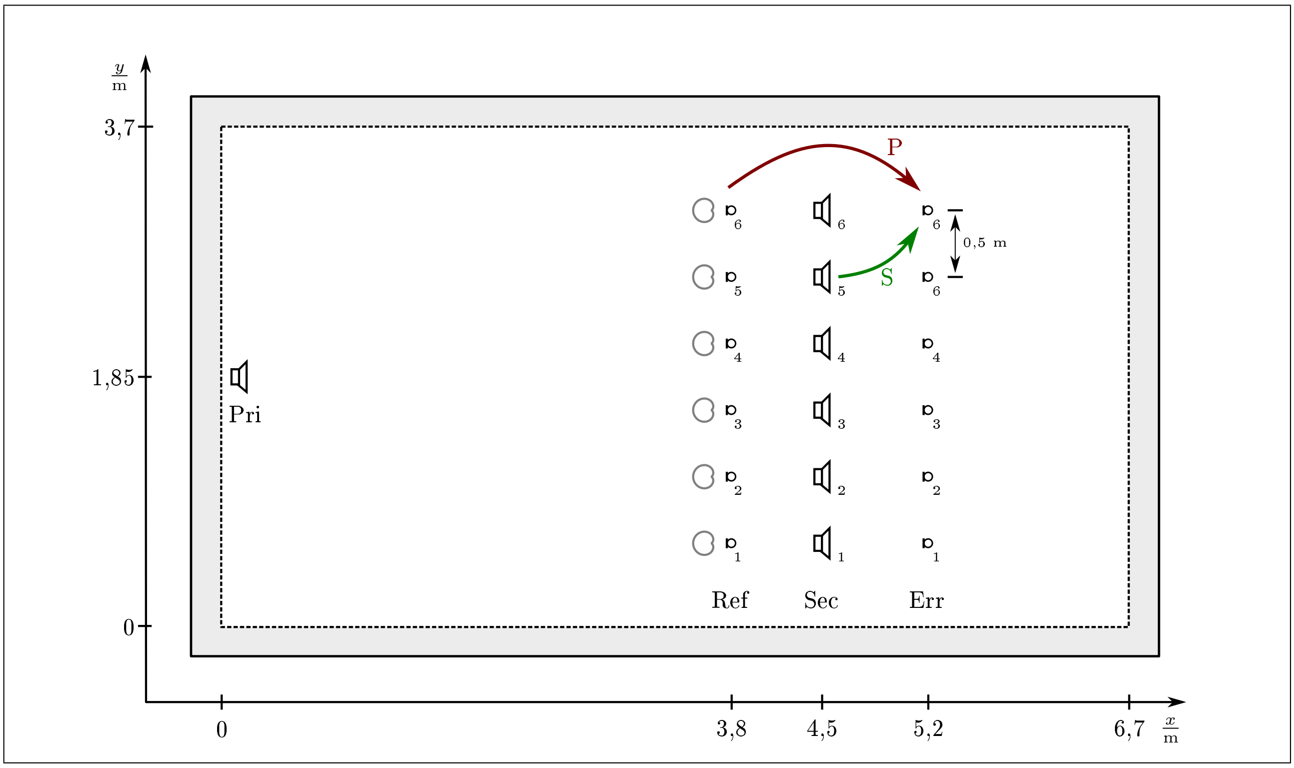

Figure 1. Geometry of the 2D MIMO ANC system in the semi-anechoic chamber of University of Wuppertal. The gray frame depicts the absorbing material. The primary source (Pri) is on the left. The cardioid reference sensors (Ref), the secondary sources (Sec) and the error sensors (Err) build the two-dimensional ANC system. The quiet zone is to the right of the secondary sources.

Figure 2. The DSK6455 DSP board with the FPGA daughter card and one OctoPre MKII Dynamic. The daughter card enables the DSP to process 24 I/O channels with 24 bit resolution and 48 kHz sampling rate by connecting three ADAT interfaces.

tencies, which are crucial in a real-time feedforward ANC system.

A new daughter card was designed to connect the three ADAT interfaces with the TMX320C6455+ DSP. It works with a Xilinx Spartan-3A-XC3S200A FPGA which converts the signals of the three ADAT channels into one serial data stream [3]. The DSP then interchanges data with the FPGA via one McBSP (Multi-channel Buffered Serial Port). The DSP can process 24 input and 24 output channels with a resolution of 24 bits and a sampling rate of 48 kHz using this daughter card. The total delay between an analog input and an analog output is 800 μs with the DSP working in loop-back mode. This value meets the requirements of the feedforward ANC approach, since the maximum delay time $\Delta t_{\max}$ is given by the shortest distance between the reference sensors and the secondary sources:

$$\Delta t_{\max} = \frac{0.7\ \mathrm{m}}{343\ \mathrm{m} \cdot \mathrm{s}^{-1}} \approx 2\ \mathrm{ms}. \tag{1}$$

The Canton CD-300 speakers and the Sonamp 1230 12 channel power amplifier that were used in the former system setup were not substituted. Only the microphone mounts have been decoupled as much as possible from the secondary sources by using microphone suspensions. In addition to that, the cantilevers that hold the microphones and which are attached to the backsides of the speakers have been strengthened. For future revisions the microphones should be totally decoupled from the loudspeakers. Behringer ECM-8000 were added to the setup s error sensors. In the past there was no error sensing.

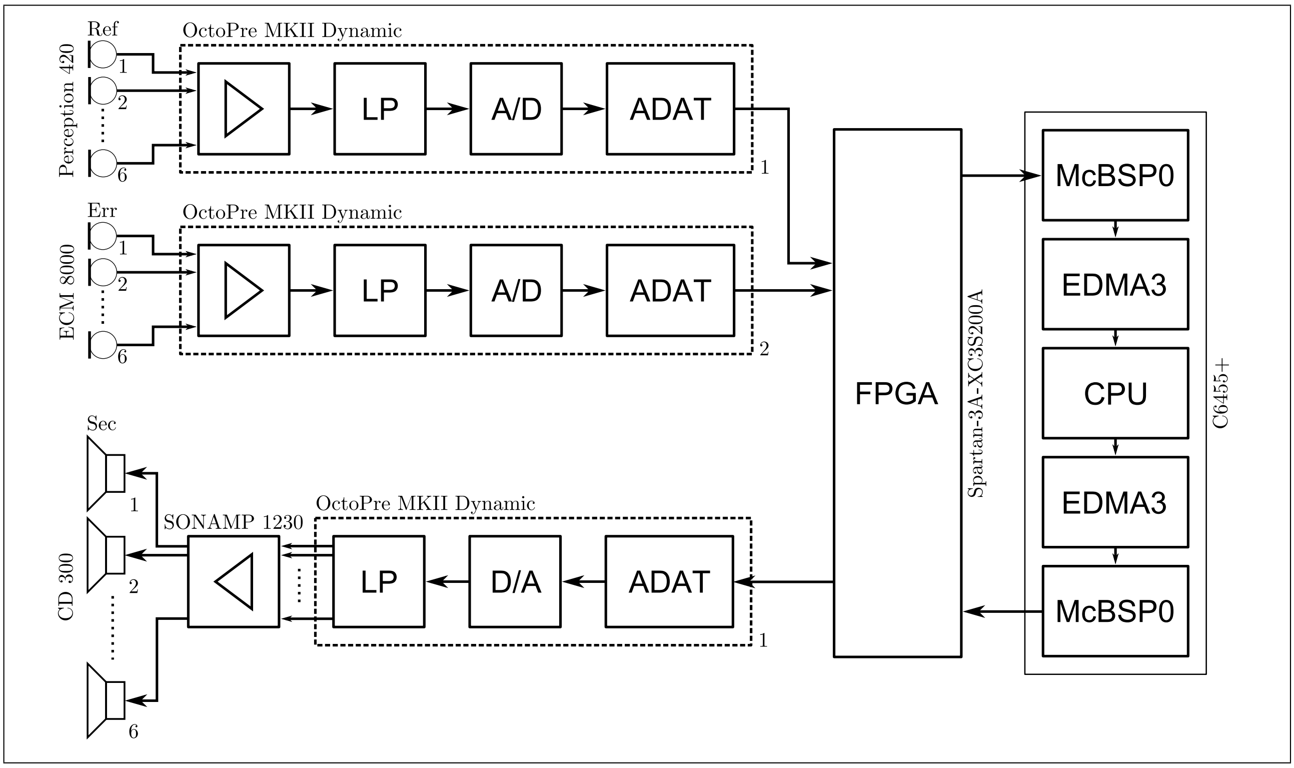

Figure 3. Signal flow of the 2D ANC system.

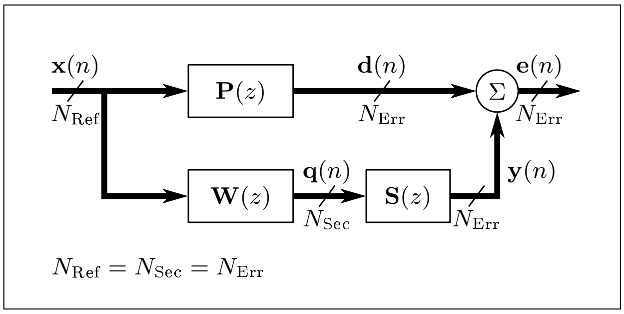

Figure 4. Simple MIMO feedforward ANC structure.

2. 2D ANC algorithms

This section gives a brief overview of the underlying 2D ANC algorithms. For further information please refer to [4].

2.1. Feedforward prediction using the Rayleigh II integral

According to figure 1 the primary paths $\mathbf{P}$ lie between the reference sensors and the error sensors. The secondary paths $\mathbf{S}$ describe the transfer paths between the secondary sources and the error sensors including all electrical components like the A/D- and D/A-converters or amplifiers [5]. An equivalent network of the MIMO system is given by figure 4 where the matrix $\mathbf{W}(z)$ describes the ANC filters in the z-domain. Obviously, an optimal MIMO filter $\mathbf{W}^{\circ}(z)$ is given by

$$\mathbf{W}^{\circ}(z) = -\mathbf{P}(z) \cdot \mathbf{S}^{-1}(z). \tag{2}$$

Therefore, the primary and the secondary paths are needed to calculate the ANC filters. The secondary paths can be measured within the system and inverted afterwards. Note, that a stable inverse $\mathbf{S}^{-1}(z)$ not necessarily exists. In practice, the primary paths can be estimated by using the two-dimensional Rayleigh II integral in combination with the cardioid microphone signals

$$P(\mathbf{r}_{\mathrm{Err}}) = \frac{jk}{2} \int_{F_0} P_{\mathrm{card}}(\mathbf{r}_{\mathrm{Ref}}) \cos\varphi H_1^{(2)}(kr)\, dF, \tag{3}$$

where $P(\mathbf{r}_{\mathrm{Err}})$ is the pressure at the error sensors, $P_{\mathrm{card}}(\mathbf{r}_{\mathrm{Ref}})$ is the pressure of the cardioid reference sensors lying on the line F_0, $k = \frac{\omega}{c}$ is the wave number, $r = |\mathbf{r}_{\mathrm{Err}} - \mathbf{r}_{\mathrm{Ref}}|$ is the distance between reference and error sensors, φ is the angle between r and the normal of F_0 and $H_1^{(2)}$ is the Hankel function of second kind.

2.2. The reflexion equivalence

An ANC system can also be regarded as a sound soft reflector or scatterer. The top of figure 5 shows a typical one-dimensional ANC setup in a pipe. On the figure's bottom an analog setup for a transmission line is

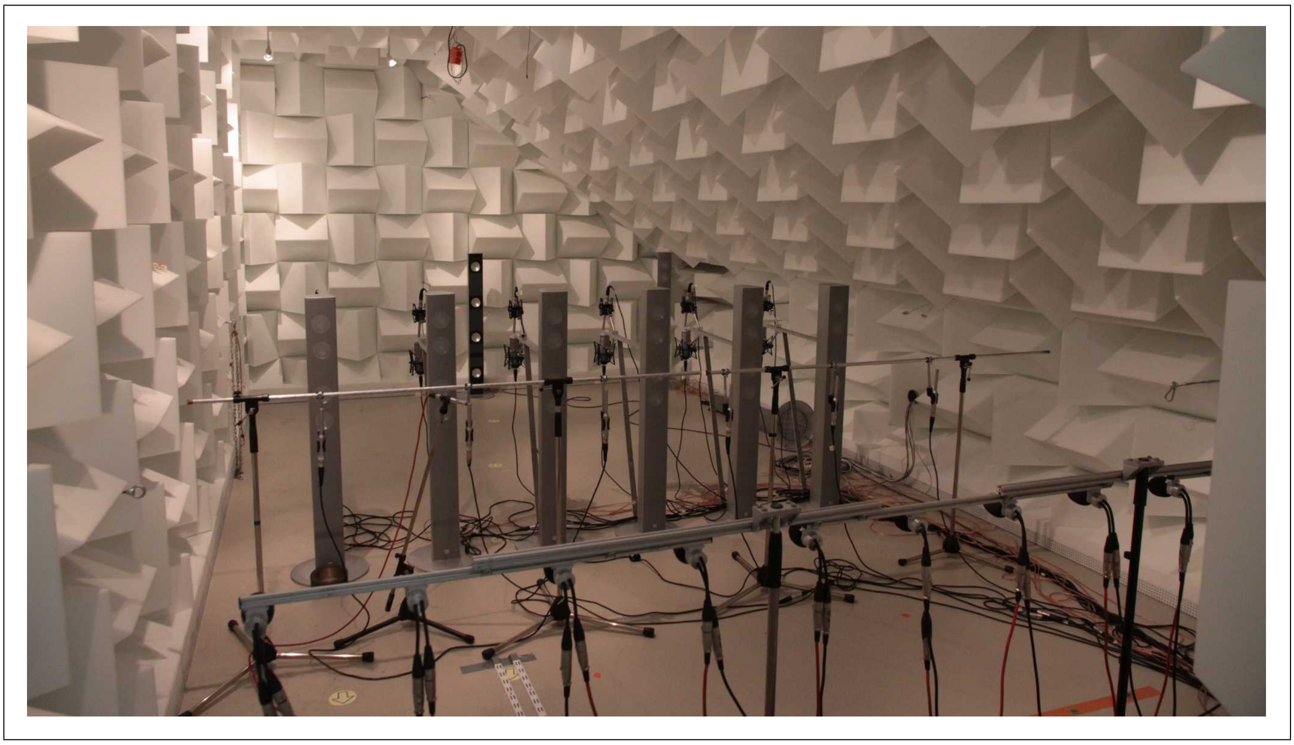

Figure 6. The MIMO ANC system in the anechoic chamber. The background shows the primary source. In the foreground the measurement system consisting of 12 microphones on a movable carrier can be seen.

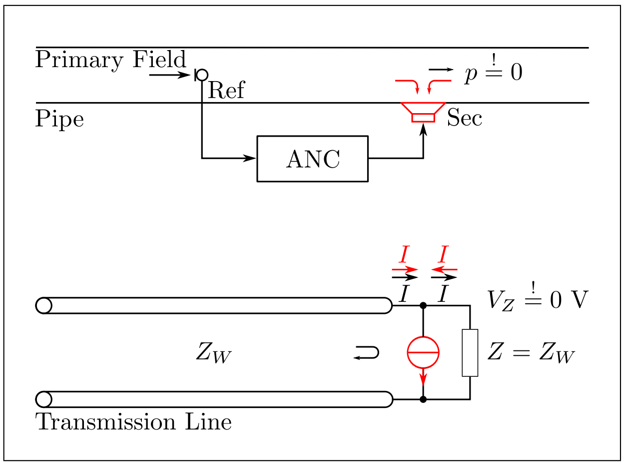

Figure 5. Reflexion equivalence in one dimension. Top: The secondary speaker of the ANC system introduces the right amount of velocity to produce a sound soft reflection with a reflectance factor of -1. Bottom: A current source introduces the current I to achieve a voltag drop of 0 V over Z and therefore the same reflectance factor.

given. In case of the transmission line a source introduces a current which has the same amount of current that would run through the impedance Z attached at the end of the line but with negative sign. This results in a zero voltage drop over the attached impedance Z and a reflectance factor of -1 as if the line was short-circuited. In case of the pipe the speaker behaves like the current source by introducing the right amount of velocity. Here, the sound pressure will be zero and the

Table I. Off-line attenuation levels at the six error microphones for band-passed noise.

Error Mic	1	2	3	4	5	6
L [dB]	20.6	23.1	21.5	18.4	20.0	22.3

velocity is two times as high as without the ANC system. Therefore, secondary source of a perfectly working ANC system behaves like a sound soft reflector.

From this perspective the ANC filters $\mathbf{W}(z)$ can be achieved directly without the knowledge of the inverse secondary paths $\mathbf{S}^{-1}(z)$. One has to assume a sound soft reflector where the secondary sources are. It is possible to use the Rayleigh II Integral in combination with Euler's equation to predict the velocity on the reflector for the line geometry. Another possibility, which also works for complex geometries and which can also take room characteristics into account, is to use a numerical simulation method like finite differences in the time domain (FDTD). The correct filters can then be taken from such simulation in which a sound soft object is implemented at the positions of the secondary sources.

2.3. MIMO FXLMS

The methods mentioned in the preceding two subsections represent open-loop control. Hence, closed-loop control can be achieved by taking into account the signals of the error sensors. Although, from a mathematical point of view, better methods for this pur-

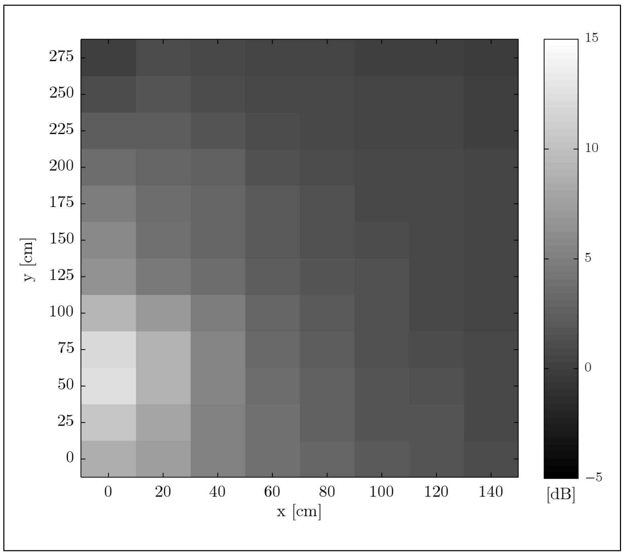

Figure 7. On-line attenuation levels in the quiet zone at a height of 0.90 meters for band-passed noise.

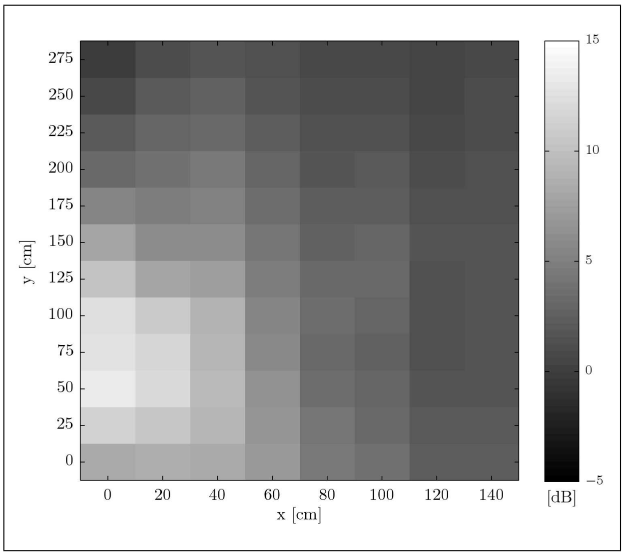

Figure 8. On-line attenuation levels in the quiet zone at a height of 1.10 meters for band-passed noise.

pose exist, the MIMO Filtered-x Least Mean Square (FXLMS) was chosen as a well known and established method for MIMO noise control. Thus, the MIMO FXLMS can be used to optimize given filter functions or to adapt optimal filters from scratch. For detailed explanation of the algorithm please refer to [5, 6, 7, 8].

3. Measurement Results

3.1. Off-line measurements

Table I shows the attenuation levels at the six error sensors for band-passed noise with the cut-off frequencies 250 Hz and 350 Hz and the stop-frequencies 200 Hz and 400 Hz. The ANC system system was running in off-line mode. This means, that the primary signal was recorded with every sensor in the system and the filter coefficients were calculated off-line using the MIMO FXLMS algorithm. Afterwards the secondary signals were uploaded to the DSP, played back synchronized with the primary source and the signals of the error microphones were recorded. The attenuation levels of table I therefore result from the ratio between the primary noise and the superposition of the primary and the secondary field. As can be seen in the table, the system is able to reduce the primary noise about 20 dB at each of the error sensors.

3.2. On-line measurements

In a second measurement the system was set to on-line mode in which the signals of the reference sensors are fed into the MIMO ANC filters to produce the secondary field in real-time. Note, that due to the utilization of cardiod reference microphones, there was no need to subtract feedback signals from the reference inputs. The on-line mode was using no further adaptation. Therefore, the off-line calculated filter coefficients where uploaded to the DSP without any more optimization during the operation of the system.

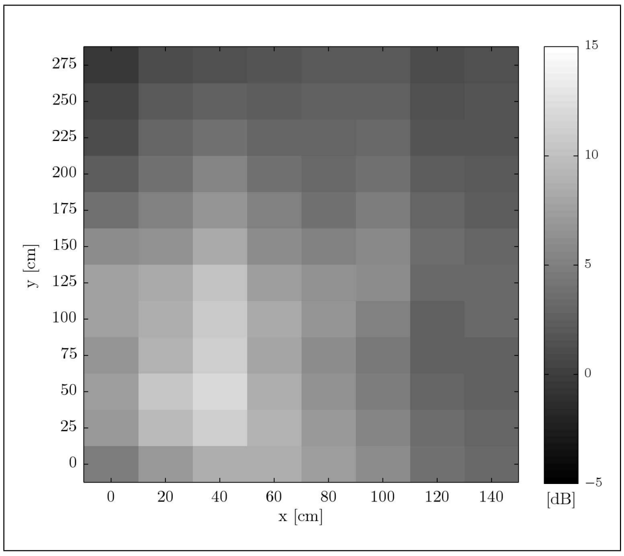

Figure 9. On-line attenuation levels in the quiet zone at a height of 1.30 meters for band-passed noise.

Figure 6 shows the system setup in the anechoic chamber. In the foreground a movable carrier with 12 microphones can be seen with which the attenuation levels in the quiet zone were measured during the on-line operation in three different heights of 0.90 m, 1.10 m and 1.30 m. For each height there have been 96 measurement points. The results are shown in figures 7, 8 and 9. The x-Positions in the figures show the distance from the error sensors. Hence, a position at $x = 0$ m is right in front of the error sensors. The y-direction basically shows the twelve measurement microphone positions. Compared with figure 6, $y = 0$ m is the leftmost and $y = 2,75$ cm is the rightmost microphone on the carrier.

The figures show less attenuation than for the off-line mode. This result could be expected since there was no further adaptation while the measurements were taken. Altogether, the measurements show that the system is running stable without feedback paths suppression and it is able to attenuate the primary field within the quiet zone. The figures also show that there is less attenuation in the vicinity of the inclined part of the ceiling. This is due to the fact, that the absorbing material doesn't really absorb within the frequency range of the primary noise which was investigated. Thus, the pitched roof area, which can be seen in the right of figure 6, reflects the primary noise into the quiet zone.

4. Conclusions

A MIMO ANC system was built by using commercially available audio equipment in combination with a TMX320C6455+ DSP. The system setup works fast enough to operate in real-time and is capable of attenuating random noise significantly. Further development will focus on the integration of on-line MIMO adaptation to achieve even better attenuation results.

References

[1] Texas Instruments. TMS320C6455 Fixed-Point Digital Signal Processor Reference Manual. SPRS276M, 2012. url: http://www.ti.com/lit/ds/symlink/tms320c6455.pdf.

[2] Spectrum Digital. DSK6455 Technical Reference Manual. C. Spectrum Digital, 2006. url: http://c6000.spectrumdigital.com/dsk6455/v2/files/6455_dsk_techref.pdf.

[3] Xilinx. Spartan-3A FPGA Family: Data Sheet. Xilinx. 2010. url: http://www.xilinx.com/support/documentation/data_sheets/ds529.pdf.

[4] C. Kleinhenrich: Aktive zweidimensionale Lärmkontrolle unter Verwendung adaptiver Verfahren und reflektierter Feldgrößen. Dissertation, University of Wuppertal, 2014.

[5] S. M. Kuo, D. R. Morgan: Active Noise Control Systems: Algorithms and DSP Implementations. John Wiley & Sons, Inc., New York, 1996.

[6] S. Elliott: Signal Processing for Active Control. Academic Press, Inc., San Diego, 2001.

[7] P. A. Nelson: Active Control of Sound. Academic Press Ltd., London, 1992.

[8] S. C. Douglas: Fast implementations of the filtered-X LMS and LMS algorithms for multichannel active noise control. IEEE Transactions on Speech and Audio Processing (7) 4 (1999) 454–465.